J. Biomechanics Vol. 17, No. 6, pp. 425–435, 1984
Printed in Great Britain

0021-9290/84 $3.00 + .00
Pergamon Press Ltd.

THE STATIC ELASTIC PROPERTIES OF 45 HUMAN THORACIC AND 20 ABDOMINAL AORTAS *IN VITRO* AND THE PARAMETERS OF A NEW MODEL

G. J. LANGEWOUTERS
Laboratory for Physiology, Free University, Amsterdam, The Netherlands

K. H. WESSELING
MFI-TNO, Utrecht, The Netherlands

and

W. J. A. GOEDHARD
BGD-TNO, The Hague, The Netherlands

Abstract—Segments of 45 human thoracic and 20 abdominal aortas, including 13 pairs, aged 30–88 yr at autopsy, were perfused with 37°C Tyrode's solution at *in-situ* length. Diameter changes due to 20 mmHg pressure steps, between 20 and 180 mmHg, were measured to 1 μm accuracy with balanced transducers. Absolute diameter at 100 mmHg was measured to 50 μm accuracy.

At 100 mmHg, cross-sectional area ranged from 2.6 to 7.6 for thoracic and from 1.0 to 3.2 cm^2 for abdominal segments. Compliances ranged from 1.9 to 17 for thoracic and from 0.6 to 4.4 mm^3/mmHg.cm for abdominal segments.

An arctangent model with three free parameters

$$A(p) = A_m(1/2 + \tan^{-1}((p - p_0)\ p_1)/\pi)$$

explained over 99% of the variance in area with pressure for each aorta. Changes in compliance, characteristic impedance and propagation velocity are equally well described.

Abdominal fits on the average appeared down scaled by a factor of 2 and shifted 20 mmHg towards lower pressures from paired thoracic (significant at $p = 0.001$).

NOMENCLATURE

A	aortic cross-sectional area
A_m	maximal area
C	aortic compliance/cm
C_m	maximal compliance/cm
d_i	internal aortic diameter
d_e	external aortic diameter
E'	incremental Young's modulus
H	height of overflow system
h	aortic wall thickness
K	coefficient of volume elasticity
L	inertance/cm
l	length of aortic segment
p	transmural pressure
p_0	max-C pressure, i.e. the pressure at which aortic compliance is maximal
p_1	half-width pressure, i.e. at $p_0 \pm p_1$ aortic compliance is equal to $C_m/2$
r	coefficient of linear correlation
r^2	coefficient of determination
r_e	external aortic radius
V	aortic volume
V_w	aortic wall volume of a segment of 10 cm length
V_p	pulse wave velocity
W	weight
Z_0	characteristic impedance
σ	Poisson ratio
ρ	density

Received 5 *July* 1983; *in revised form* 5 *October* 1983.
Address for reprints: Dr. G. J. Langewouters, Biomedical Instrumentation Research Unit TNO, Academisch Medisch Centrum (AMC), Meibergdreef 9, 1105 AZ Amsterdam, The Netherlands.

INTRODUCTION

Much work has been done to determine the static and dynamic mechanical properties of arteries, as witnessed by a number of reviews (Reuterwall, 1921; Kapal, 1954; Sinn, 1956; Bergel, 1960, 1972; Bader, 1963; Remington, 1963; Kenner, 1967; Wetterer and Kenner, 1968; Fung, 1972, 1973; Dobrin, 1978 and Yin, 1980). Most of the current knowledge, by far, is from studies on blood vessels of animals. Studies on *human* blood vessels are scarce, with controversial results and interpretations. We therefore studied human aortic segments *in vitro*:

(1) with measurement conditions controlled closely and near physiological on the points of temperature of the perfusate and tone of the smooth muscle;

(2) using techniques sufficiently accurate to be able to apply parameter estimation techniques to individual aortas, not to averages;

(3) measuring dynamic mechanical properties as a function of arterial pressure, not at or near only a single pressure level (to be reported in a subsequent paper);

(4) over a wide age range with special emphasis on old aortas about which little or no information is available.

MATERIALS AND METHODS

Material

Human aortic segments were obtained at autopsy in two Amsterdam hospitals: the Onze Lieve Vrouwe Gasthuis (OLVG) and the Academisch Ziekenhuis der Vrije Universiteit (AZVU). Straight segments of almost uniform diameter and without large side branches were chosen from two sites as follows:

(1) 10 cm of the descending thoracic aorta just above the diaphragm, subsequently called 'thoracic aorta', and/or

(2) 6 cm of the abdominal aorta from between the renal arteries and the iliac bifurcation, subsequently called 'abdominal aorta'.

After excision the segments were stored in a thermos bottle filled with glucose-free Tyrode's solution at 4°C. We measured 45 thoracic and 20 abdominal aortas; pairs were obtained from 13 subjects.

Before measurement all loose connective tissue was removed while care was taken to leave all side branches intact. Upon later histological examination of the vessel segments remnants of the adventitia were seen on stained sections, indicating that the tunica media was left intact.

Retraction was determined by measuring the distance between two points on the isolated vessel under zero transmural pressure. These points had been previously marked *in-situ* at a known distance. The segment was next suspended on a Mettler balance to measure the wall volume. The segment was weighed twice: in air (weight W_1) and in Tyrode (weight W_2). The wall volume, V_w, of the segment then follows as

$$V_w = \frac{W_1 - W_2}{\rho_T} \tag{1}$$

where ρ_T (= 1060 kg m^{-3}) is the density of Tyrode. Finally, the segment was cannulated at both ends using perspex connectors of suitable diameter and mounted in the measurement apparatus, stretched at its precise *in-situ* length.

Methods

A schematic drawing of the measurement apparatus is shown in Fig. 1. A blood vessel segment was mounted horizontally in the apparatus. One connector was put in a fixed support coupled to pressure reservoir 1 via a variable hydraulic resistance (VR1) (Westerhof *et al.*, 1971) and a bidirectional combination of two fast hydraulic valves (V1 and V2) designed to open in less than 2 ms (Wesseling *et al.*, 1978). The connector at the other end of the segment was coupled to a second pressure reservoir (2) via a glass tube in a movable support and another hydraulic resistance (VR2). A

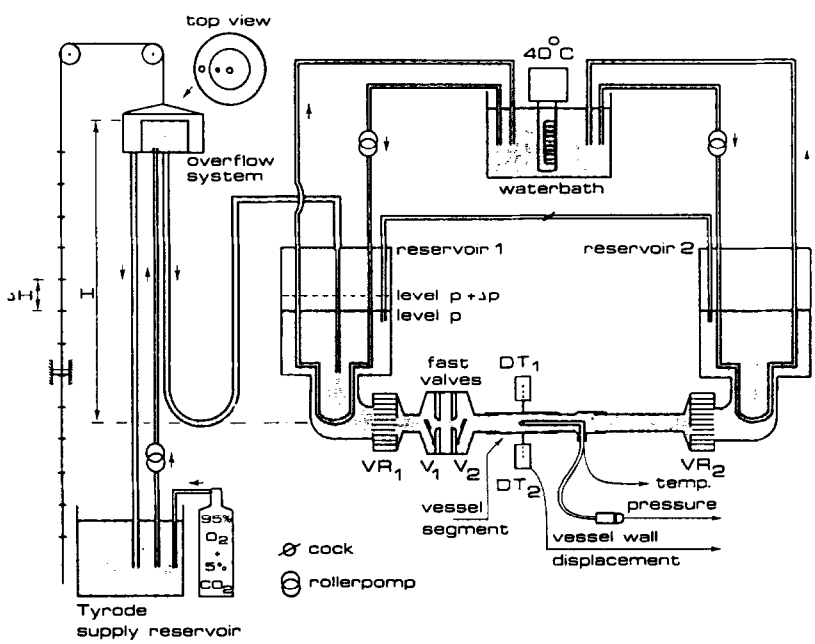

Fig. 1. Schematic drawing of the apparatus in which the pressure–diameter relationship of human aortic segments *in vitro* was measured. A vessel segment is perfused with oxygenated Tyrode's solution from the supply reservoir. Pressure in the vessel segment depends on the hydrostatic height, H, of the overflow system. Pressure can be changed (up and down) in steps of 20 mmHg, by means of the adjustable height of the overflow system in combination with the fast valves (V1 and V2). The resulting changes in the segment's external diameter are measured with a balanced arrangement of two displacement transducers (DT1 and DT2). The temperature of the fluid inside the vessel segment is kept constant at 37 ± 1°C. For further explanations see text.

stainless steel tube (1 mm bore, 15 cm long), with a side hole near its tip was cemented into the glass tube. The tip was situated about the midpoint of the vessel segment and coupled to a Statham P23Db pressure transducer. The tube tip was also fitted with a thermistor measuring the temperature of the liquid.

Aortic segments were perfused with Tyrode's solution, continually aerated with a mixture of 95 % O_2 and 5 % CO_2. The pH of the solution was equal to the pH of normal blood: 7.4 ± 0.1. The temperature of the Tyrode was regulated to 37 ± 1 °C by means of heater coil through which hot water was pumped. The outside of the aortic segments was kept wet with Tyrode of the same temperature.

Pressure in the aortic segments was varied by supplying Tyrode to reservoir 1 via an overflow system of which the height, H, could be varied at preset levels corresponding to 20 mmHg (2.67 kPa) pressure increments up to a maximum transmural pressure of 180 mmHg (24 kPa). A step pressure change in the aortic segment was generated in the following manner. At a given stable pressure level, p, maintained by reservoir 2, the cock and valve V2 were closed, and the height of the overflow system was raised by one increment. Upon the release of valve V2, the pressure in the aortic segment was increased stepwise one increment. Downwards pressure steps could be generated in similar fashion with the other valve V1. With this system we were able to obtain rise-times of less than 50 ms for the pressure in the middle of the aortic segments, which is about as fast as aortic pressure rises in systole.

Diameter changes of the aortic segments were measured precisely at the site of the pressure measurement using a balanced arrangement of two identical displacement transducers (SE-Labs, type 351), each having a linear calibrated stroke of ± 5 mm. A balanced arrangement was necessary since some vessels decreased their bending radius with increasing pressure, thus invalidating one-sided measurements. A sketch of the arrangement is shown in Fig. 2. The balanced transducer output was linear with actual displacement to within 0.2 %, as was estimated from calibration curves after linear least squares regression analysis. Diameter changes up to ± 10 mm could thus be measured with an accuracy of better than 1 μm.

An X-ray picture of a vessel segment and its connectors of known dimensions, made at a pressure level of 100 mmHg, provided the reference external diameter, which was measured from the X-ray picture with a vernier caliper with an accuracy of ± 0.05 mm.

After placement in the measurement apparatus, a segment was allowed to accomodate for at least one hour at 100 mmHg. Next the segment was conditioned by slowly inflating, then deflating the segment between 20 and 180 mmHg at a rate of about 1 mmHg s^{-1} to remove passive smooth muscle tone (Cox, 1975). A 'stable' pressure-diameter hysteresis-loop was usually obtained after three to five inflation–deflation cycles as found by others (Remington, 1955; Bergel, 1961a; Fung, 1967; Cox, 1975). Pressure was then increased in 20 mmHg steps from 20 to 180 mmHg and deflated similarly (see Fig. 3). Beginning just before a pressure step, diameter changes were recorded until at least 50 s after the onset of the pressure step. After this period the vessel diameter usually remained stable to within 1 μm. The signals were recorded on a 4-channel HP2695 instrumentation recorder for later processing.

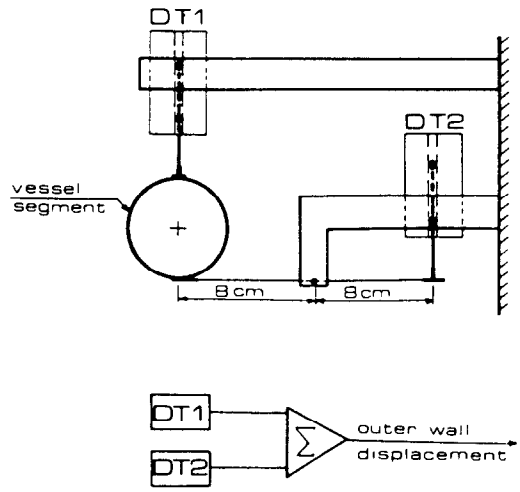

Fig. 2. Details of the balanced arrangement for measuring diameter changes. The transducers DT1 and DT2 can be adjusted independently in a vertical direction to allow a proper adjustment of each transducer to within its linear range.

The internal cross-sectional area, A, of a vessel segment with measured length l, wall volume V_w and external diameter d_e was computed as

$$A = \frac{\pi}{4} d_e^2 - \frac{V_w}{l}. \quad (2)$$

The external diameter was computed at intervals of 20 mmHg from the reference external diameter (X-ray at 100 mmHg) and the measured displacement data. The error from all sources in the computed cross-sectional area varied from ± 0.025 cm^2 (2 %) for the smaller vessels at low pressure (d_e = 1.5 cm) to ± 0.07 cm^2

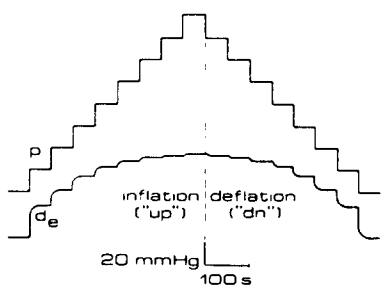

Fig. 3. A complete measurement cycle. The pressure in the segment was first increased from 20 to 180 mmHg in steps of 20 mmHg. The resulting increase in the segment's diameter, d_e, becomes smaller with each step. Then the pressure was stepped in the opposite direction back to 20 mmHg.

(0.8%) for the larger vessels at high pressure (d_e = 3.75 cm). The greater part of the error is due to the inaccuracy of the reference external diameter ($\pm 50\,\mu$m); the changes in diameter were measured with much higher precision (better than 1 μm).

The resulting pressure–area diagrams appear as smooth monotonous curves. A simple relationship fits the p–A diagram (Langewouters *et al.*, 1981; Langewouters, 1982) as follows

$$A(p) = A_m \left\{ \frac{1}{2} + \frac{1}{\pi} \tan^{-1} \left(\frac{p - p_0}{p_1} \right) \right\} \tag{3}$$

in which A_m, p_0 and p_1 are three independent parameters to be estimated for each segment.

The model is based on the observation that the incremental Young's modulus (or reciprocal compliance) increases with pressure according to a second order function (Wetterer and Kenner, 1968 and our data)

$$E' \sim \frac{1}{C} = \frac{dp}{dA} = a + bp + cp^2. \tag{3a}$$

By algebraic manipulation this equation can be rewritten as follows

$$dA = \frac{A_1 . dp}{1 + \left(\frac{p - p_0}{p_1} \right)^2}. \tag{3b}$$

Integration yields

$$A = A_1 . \tan^{-1} \left(\frac{p - p_0}{p_1} \right) + A_2. \tag{3c}$$

The boundary condition $A(p = -\infty) = 0$ yields: $A_2 = \pi A_1/2$.

The 'static' compliance of the aorta can be defined as the derivative of equation (3) with respect to pressure

$$C(p) = \frac{C_m}{1 + \left(\frac{p - p_0}{p_1} \right)^2}; \quad C_m = \frac{A_m}{\pi p_1}. \tag{4}$$

These functions are shown, fitted to a set of typical measurement points, in Fig. 4. Parameter A_m is the maximum cross-sectional area of the aorta at high pressures, further called 'maximal area'. Parameter p_0 is the transmural pressure at the inflection point in the pressure–area curve. At this pressure level the compliance curve reaches its maximum, C_m. Therefore, p_0 is further called 'max-C-pressure'. Parameter p_1 represents the steepness of rise of the curve and therefore compliance. At pressure levels $p_0 \pm p_1$ the compliance of the vessel is reduced to one-half of its maximum value. Thus p_1 is termed 'half-width pressure'.

The Marquardt procedure (Marquardt, 1963; Horwitz and Homer, 1970) was used to least squares fit the function to the individual data, giving estimates for the parameters A_m, p_0 and p_1 for each segment.

Characteristic impedance, Z_0, and pulse wave velocity, V_p, were computed at each pressure level with the following approximate formulae

$$Z_0 = \sqrt{\frac{L}{C}} = \sqrt{\frac{\rho}{A} \cdot \frac{\Delta p}{\Delta A}} \tag{5}$$

$$V_p = \sqrt{\frac{1}{LC}} = \sqrt{\frac{A}{\rho} \cdot \frac{\Delta p}{\Delta A}} \tag{6}$$

$$L = \rho/A; \quad C = \frac{\Delta A}{\Delta p} \tag{7}$$

in which ρ is the density of the liquid filling the segment (blood), L is the inertance and C is the compliance of the vessel per unit length. In this paper Z_0 is expressed

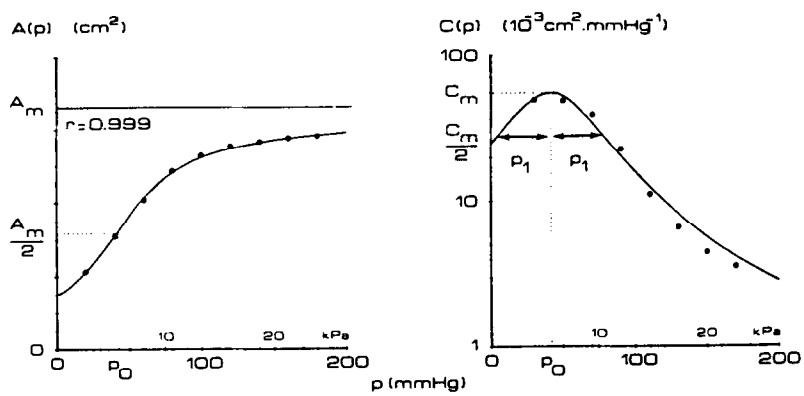

Fig. 4. Aortic cross-sectional area, $A(p)$, and aortic compliance, $C(p)$, over the pressure range 0–200 mmHg. The solid line in the left-hand panel is the graphical representation of the arctangent function of equation (3), when least squares fitted to the measurements. Substitution of the parameter values for A_m, p_0 and p_1 in equation (4) gives the aortic compliance as a function of pressure, represented by the solid line in the right-hand panel. The dots refer to the compliance values computed from the measured pressure–area data, at pressure levels from 30 to 170 mmHg.

in mmHg s cm^{-3} (N s m^{-5}) and V_p in m s^{-1}. Since the static compliance was used for Z_0 and V_p, this leads to values perhaps some 10–15% lower than if the dynamic compliance were used, because the dynamic compliance is some 20–30% smaller than the static compliance (Bergel, 1961b; Learoyd and Taylor, 1966).

The incremental Young's modulus, E', is computed from the measurements as

$$E' = 2(1-\sigma^2)\frac{d_i^2 d_e}{d_e^2 - d_i^2}\frac{\Delta p}{\Delta d_e} \qquad (8)$$

in which σ is the poisson ratio ($\sigma = 0.5$ for incompressible materials such as the aortic wall), d_i is the internal diameter of the vessel, d_e is the external diameter, Δp is the pressure increment and Δd_e is the resulting increment in the external diameter of the aorta (Krafka, 1939; Bergel, 1960). Putting $\sigma = 0.5$ and using equation (2) this can be rewritten as

$$E' = 3\frac{A.1 + V_w}{V_w}\left(A\frac{\Delta p}{\Delta A}\right). \qquad (9)$$

The formula is valid for homogeneous, isotropic, piece-wise linear, purely elastic materials with a cylindrical cross-section. Thus application to aortas is a gross approximation.

RESULTS

Figure 5 shows representative experimental data for a segment of human thoracic aorta. 'Up' and 'dn' indicate the direction in which the pressure was changed. Moderate hysteresis is seen to be present, with the differences in corresponding areas less than 2%.

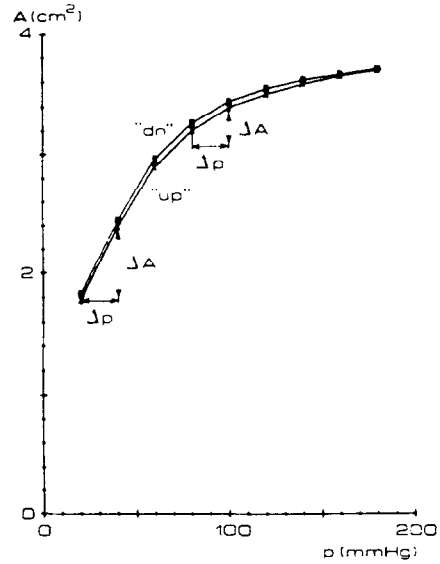

Fig. 5. Static relationship between pressure and cross-sectional area of the thoracic aorta of a 45 yr old female (no. 78111). The cross-sectional area of the segment upon inflation is slightly smaller than that during deflation, giving rise to a small hysteresis loop in the pressure–area diagram.

Dimensions of the thoracic and abdominal aortas at 100 mmHg inflation pressure are listed in Table 1. The

Table 1. Dimensions and other data of 45 individual segments of human thoracic and 20 abdominal aorta of which 13, marked with a dot, are pairs from the same subject. The aortas are grouped in age decades. The bottom line histograms give an impression of the distributions involved. Delay = time in hours between autopsy and experiment; retr = retraction; V_w = wall volume of an equivalent segment of 10 cm length; d_e = external diameter at 100 mmHg; h = wall-thickness at 100 mmHg; A = aortic cross-sectional area at 100 mmHg; C = aortic compliance at 100 mmHg

THORACIC AORTA

patient no.	age years	delay hours	retr. %	V_w cm³	d_e cm	h cm	A cm²	C 10^{-3} cm²/mmHg
• 78067	30	95	8.0	8.90	2.16	0.14	2.77	12.39
• 78003	39	27	15.0	10.64	2.85	0.12	5.29	16.61
77264	45	23	10.0	10.00	2.49	0.14	3.85	9.57
78111	45	28	8.0	8.74	2.33	0.13	3.39	7.51
• 78094	46	29	6.0	10.11	2.15	0.16	2.63	5.52
78098	47	4	8.0	9.20	2.64	0.12	4.54	12.60
• 77278	50	3	7.0	11.68	2.49	0.16	3.69	11.94
78054	50	6	8.0	10.58	2.30	0.16	3.11	4.18
78080	50	26	6.0	10.34	2.49	0.14	3.84	4.88
• 78009	53	28	7.0	12.23	2.80	0.15	4.94	9.36
• 4079	54	56	13.3	11.08	2.40	0.16	3.42	4.94
78065	56	24	8.0	10.07	2.48	0.14	3.82	5.77
3972	57	28	3.3	16.12	2.83	0.20	4.66	8.41
• 77266	57	46	5.0	11.04	2.16	0.18	2.56	3.22
78173	58	77	6.0	12.53	2.81	0.15	4.95	7.10
• 77207	59	27	8.0	11.80	2.54	0.16	3.89	4.86
78063	60	29	0.5	19.71	2.85	0.24	4.42	5.86
78018	63	29	4.0	11.97	2.69	0.15	4.50	8.89
• 78048	64	49	6.0	10.97	2.49	0.23	3.77	4.40
3942	65	24	7.0	20.11	3.00	0.23	5.06	8.23
• 77286	66	7	3.0	14.23	2.59	0.19	3.83	3.52
77291	66	94	2.0	14.66	2.83	0.18	4.81	5.60
77296	66	28	6.0	17.50	3.23	0.18	6.44	8.97
78051	66	68	5.0	15.62	2.71	0.20	4.19	5.19
3938	68	14	5.0	13.62	2.54	0.18	3.72	5.81
4020	68	6	5.0	17.38	2.70	0.22	4.30	3.07
3943	71	6	5.0	18.36	3.07	0.20	5.55	7.18
78032	71	98	4.0	21.75	3.16	0.24	5.67	4.45
4097	72	96	2.0	13.11	3.52	0.18	3.47	3.48
78174	72	99	5.0	20.55	3.04	0.23	5.22	5.55
• 77196	73	26	0.2	18.33	2.83	0.22	4.45	4.44
78185	75	27	3.0	12.55	2.66	0.16	4.31	1.87
4088	76	24	2.0	21.47	3.21	0.23	5.97	3.41
• 77292	76	71	0.2	14.22	2.41	0.21	3.15	3.17
• 77297	76	22	3.0	16.17	2.62	0.21	3.76	3.33
77268	79	72	0.2	25.89	3.26	0.28	5.75	4.12
77267	80	30	2.0	14.26	2.55	0.19	3.67	3.30
77285	81	72	2.0	19.75	3.49	0.19	7.57	5.65
77271	82	25	3.0	16.71	2.79	0.21	4.46	2.34
4023	85	48	4.0	15.35	3.00	0.17	5.53	3.14
4071	85	6	-0.1	19.44	2.76	0.25	4.04	4.22
3971	87	5	0.3	37.89	3.34	0.41	4.96	3.54
77293	87	49	0.1	26.70	3.27	0.29	5.71	2.98
77213	88	27	0.2	15.63	2.76	0.19	4.42	4.44
77289	88	27	-0.0	18.10	3.15	0.20	5.97	5.10

ABDOMINAL AORTA

patient no.	age years	delay hours	retr. %	V_w cm³	d_e cm	h cm	A cm²	C 10^{-3} cm²/mmHg
• 78067	30	121	8.0	7.89	1.68	0.17	1.43	4.05
• 78003	39	29	15.0	8.62	2.20	0.13	2.93	4.15
78107	40	28	12.0	5.66	1.60	0.12	1.43	2.06
• 78094	46	50	6.0	6.92	1.58	0.15	1.28	1.41
78119	46	27	10.0	7.62	1.94	0.13	2.29	1.96
• 77278	50	72	7.0	7.67	1.83	0.15	1.65	2.13
• 78009	53	50	7.0	11.43	2.36	0.17	3.22	2.63
• 4079	54	29	6.0	9.00	1.81	0.18	1.97	2.03
• 77266	57	71	5.0	8.14	1.54	0.19	1.24	1.03
78023	58	6	8.0	8.70	1.97	0.15	2.17	1.20
• 77207	59	31	8.0	7.90	1.70	0.16	1.47	1.40
78052	63	29	5.0	9.98	2.23	0.15	2.47	2.40
• 78048	64	49	6.0	6.72	1.66	0.14	1.45	1.54
• 77286	66	27	3.0	10.12	1.85	0.23	1.97	1.28
78060	70	31	4.0	9.74	2.07	0.16	2.38	1.46
• 77196	73	48	0.2	17.55	2.10	0.31	1.75	1.03
78180	75	27	3.0	14.74	2.05	0.26	1.84	1.07
• 77292	76	73	3.1	10.00	1.72	0.21	1.33	1.14
• 77297	76	45	3.0	10.43	1.81	0.21	1.53	0.60
78047	78	25	5.0	8.41	1.81	0.16	1.76	1.18

range of internal cross-sectional area, A, of the individual aortas is: thoracic from 2.6 to 7.6 cm^2; abdominal from 1 to 3.2 cm^2. The slopes of the individual pressure–area curves are also substantially different; consequently, compliance values at 100 mmHg range from 1.9 to 16.6 10^{-3} cm^2 $mmHg^{-1}$ (14–124 cm^2 Pa^{-1}) for the thoracic aorta and from 0.6 to 4.4 10^{-3} cm^2 $mmHg^{-1}$ (4.5–33 cm^2 Pa^{-1}) for the abdominal aorta.

Linear regressions of the abdominal upon the 13 paired thoracic values for A and C at 100 mmHg are shown in Fig. 6. The internal cross-sectional area of the abdominal aorta is about one half of the thoracic value. Abdominal compliance is about one quarter of the thoracic value.

Table 2 summarizes the Marquardt arctangent model parameter estimates for the maximal area, A_m, the max-C pressure, p_0, and the half-width pressure, p_1, as obtained from the pressure–area measurements. The coefficient of determination, r^2, is very nearly 1 ($r^2 > 0.991$) and the SEE less than 2% of A_m for all aortic segments, indicating agreement between measure-

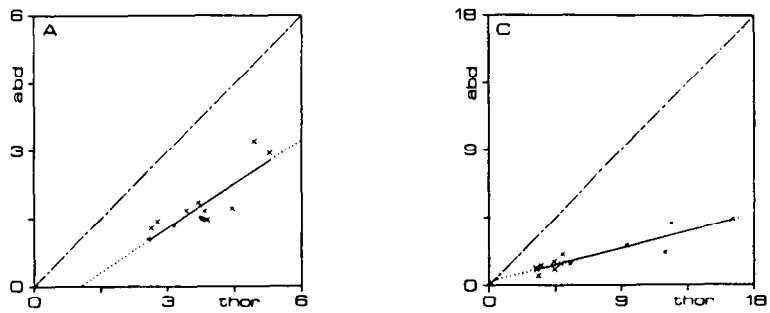

Fig. 6. Internal cross-sectional area, A (cm^2), and compliance, C (10^{-3} cm^2 $mmHg^{-1}$), of the abdominal aorta at 100 mmHg vs the thoracic values (13 pairs) and the linear regressions (solid lines). Dashed lines are lines of identity. The regression equations are: $A_{abd} = -0.68 + 0.65^* A_{thor}$, $r = 0.86$ ($p < 0.001$), $SEE = 0.34$ $C_{abd} = 0.25 + 0.24^* C_{thor}$, $r = 0.92$ ($p < 0.001$), $SEE = 0.47$.

Table 2. Estimates of the individual arctangent model parameters. The measurement data upon inflation are used. A_m = maximal area; p_0 = max-C pressure; p_1 = half-width pressure; r^2 = coefficient of determination; SEE = standard error estimate

THORACIC AORTA

patient nr.	age years	A_m cm^2	P_0 mmHg	P_1 mmHg	r^2	SEE (cm^2)
• 78067	30	3.50	50.4	42.3	0.9980	0.040
• 78003	39	6.37	41.3	36.8	0.9992	0.040
77264	45	4.59	36.5	36.0	0.9996	0.018
78111	45	4.02	27.7	39.7	0.9998	0.009
• 78094	46	3.13	24.9	41.0	1.0000	0.004
78098	47	5.52	31.7	44.4	0.9994	0.024
• 77278	50	4.61	38.5	45.7	0.9996	0.019
78054	50	3.51	20.3	32.1	0.9970	0.030
78080	50	4.32	26.0	29.6	0.9954	0.056
• 78009	53	5.74	27.1	36.8	0.9980	0.041
• 4079	54	3.87	23.9	29.4	0.9996	0.016
78065	56	4.35	25.7	33.2	0.9956	0.054
3972	57	5.31	29.5	28.8	0.9998	0.006
• 77266	57	2.84	21.4	26.0	0.9996	0.010
78173	58	5.61	21.1	31.5	0.9990	0.030
• 77207	59	4.34	18.3	26.7	0.9998	0.010
78063	60	4.97	21.2	29.5	0.9982	0.036
78018	63	5.25	25.7	38.8	0.9964	0.058
• 78048	64	4.18	12.7	28.0	0.9998	0.007
3942	65	5.76	23.4	30.7	1.0000	0.010
• 77286	66	4.17	12.2	22.2	0.9994	0.013
77291	66	5.33	18.7	27.9	0.9978	0.041
77296	66	7.27	19.6	30.1	0.9998	0.019
78051	66	4.65	15.9	27.0	1.0000	0.006
3938	68	4.26	20.3	35.0	0.9990	0.023
4020	68	4.28	5.5	19.4	0.9992	0.012
78032	71	6.30	16.4	27.1	1.0000	0.004
3943	71	5.94	11.4	17.1	0.9976	0.040
4097	72	4.00	12.6	23.1	0.9996	0.011
78174	72	5.75	6.5	27.1	0.9980	0.020
• 77196	73	4.90	11.6	26.0	0.9996	0.015
78185	75	4.51	-1.1	13.1	0.9992	0.008
4088	76	6.31	2.1	15.9	0.9988	0.017
• 77292	76	3.50	2.1	29.6	0.9986	0.014
• 77297	76	4.09	7.7	23.0	0.9998	0.007
77268	79	6.18	-2.3	21.6	0.9992	0.014
77267	80	3.88	-11.7	18.5	0.9960	0.013
77285	81	8.10	3.7	18.9	0.9986	0.027
77271	82	4.74	-14.4	20.7	0.9974	0.013
4023	85	5.83	1.8	15.1	0.9974	0.022
4071	85	4.45	10.8	26.3	0.9998	0.007
3971	87	5.32	-0.4	20.7	0.9990	0.013
77293	87	6.01	1.1	14.4	0.9984	0.017
77213	88	4.89	-0.4	29.5	0.9980	0.021
77289	88	6.48	1.3	23.1	0.9958	0.038

ABDOMINAL AORTA

patient nr.	age years	A_m cm^2	P_0 mmHg	P_1 mmHg	r^2	SEE (cm^2)
• 78067	30	1.73	33.3	35.7	0.9986	0.015
• 78003	39	3.39	21.5	27.4	1.0000	0.038
78107	40	1.62	19.0	31.9	0.9990	0.016
• 78094	46	1.41	11.7	26.1	0.9996	0.017
78119	46	2.38	12.9	21.4	0.9998	0.035
• 77278	50	2.06	9.0	29.1	1.0000	0.022
• 78009	53	3.47	7.5	20.5	0.9994	0.054
• 4079	54	1.88	8.6	29.3	0.9990	0.020
• 77266	57	1.15	1.8	26.6	0.9996	0.013
78023	58	2.36	-2.0	24.3	0.9972	0.030
• 77207	59	1.63	-4.4	31.5	0.9982	0.016
78052	63	3.14	-0.5	23.7	0.9994	0.042
• 78048	64	1.62	8.1	25.0	0.9996	0.020
• 77286	66	1.79	8.3	20.0	0.9998	0.028
78060	70	2.54	-5.8	20.4	0.9986	0.039
• 77196	73	1.84	-18.7	22.8	0.9998	0.025
78180	75	1.98	-29.2	28.5	0.9958	0.022
• 77292	76	1.47	-16.9	33.6	0.9992	0.014
• 77297	76	1.62	-40.3	21.7	0.9992	0.021
78047	78	1.87	-7.7	24.7	0.9994	0.024

ments and model within the experimental accuracy (see Fig. 4 for a typical result). The estimated max-C pressure, p_0, is sometimes less than the lower limit of measurement of 20 mmHg.

Linear regression analysis of the abdominal upon the paired thoracic parameters A_m, p_0 and p_1 are shown in Fig. 7. The figure shows that the maximal area, A_m, of the abdominal aorta is about one-half of the paired thoracic value. For p_0 the figure shows that the abdominal differs from the thoracic value by about 20 mmHg (2.67 kPa). For p_1 no relationship is apparent.

Results of a comparison between inflation and deflation experiments are summarized in Table 3. The differences between the parameters are small and physiologically unimportant. Statistically they are highly significant in most cases and seem systematic in nature.

The characteristic impedance, Z_0, the pulse wave velocity, V_p, and the static incremental Young's modulus, E', derived from the measurements and from the particular arctangent model for a typical thoracic aortic segment (no. 78003) are shown in Fig. 8. The model curves for Z_0, V_p and E' are computed from the model for the cross-sectional area, A, and are thus not fits to their own data points. Nevertheless, the agreement is close. Table 4 lists the values of these quantities derived from the measurements at a pressure level of 100 mmHg.

Figure 9 depicts the 13 paired thoracic-abdominal comparisons for Z_0, V_p and E' at 100 mmHg. The Z_0 for the abdominal aorta is about three times that of the thoracic aorta. The velocity of propagation, V_p, is approximately 2.5 m s^{-1} higher in the abdominal aorta. For E' no relationship is apparent.

DISCUSSION

The loading of the vessel wall by the weight of the armature of the displacement transducers (0.07g) theoretically causes indentation of the vessel wall and deformation of the vessel's cross-section towards ellipsoidal, thus biasing the d_e measurements. We studied this possible effect by comparing the displacement transducer method with a non-contacting impedance-rheographic method (Geddes and Baker, 1968) on a rubber tube with a modulus of elasticity of about 1.0 10^5 Nm^{-2}, close to that of an aorta at low pressure where effects should be most noticeable. The dimensions and dimension changes with time were measured simultaneously by both methods. Data obtained by the displacement transducers agreed with those obtained by impedance-rheography to within the experimental accuracy estimated at 1 % or 0.02 cm^2 for each method. In fact differences were not observable. From these experiments it was concluded that the influence of loading the aortic segments with the weight of the displacement transducer on measurement error is negligible.

Further errors can arise from the following sources

(1) non-uniformity of the aortic wall, amplified by the presence of atherosclerotic lesions;

(2) the presence of side-branches, giving rise to irregularities in the external vessel diameter;

(3) natural curvature of the aortic segments;

(4) end-effects due to cannulation of the segments.

The assumption that arteries are regular circular cylinders which expand uniformly when inflated is dubious. We tried to minimize errors due to these sources by selecting segments which appeared to be

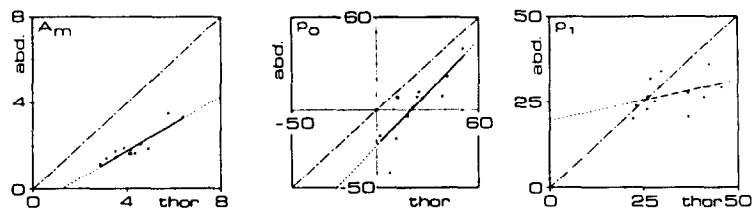

Fig. 7. Maximal area, A_m (cm^2), max-C pressure, p_0 (mmHg) and half-width pressure, p_1 (mmHg), for the abdominal aorta vs the thoracic values (13 pairs) and the linear regressions (solid lines). Dashed lines are lines of identity. The regression equations are: $A_{m\,abd} = -0.75 + 0.63^* A_{m\,thor}$, $r = 0.91$ ($p < 0.001$), $SEE = 0.3$ $p_{0\,abd} = -22.8 + 1.13^* p_{0\,thor}$, $r = 0.81$ ($p < 0.001$), $SEE = 12.0$, $p_{1\,abd} = 19.6 + 0.23^* p_{1\,thor}$, $r = 0.38$ (NS), $SEE = 4.6$.

Table 3. Comparison of the parameters A_m, p_0, p_1 and C_m as obtained from inflation (up) and deflation (dn) experiments on human thoracic and abdominal aortas. (* = $p < 0.05$; † = $p < 0.001$; NS = not significant at $p = 0.05$)

Parameter	up-dn	Thoracic aorta $N = 45$ Mean	S.D.	Significance	Abdominal aorta $N = 17$ Mean	S.D.	Significance
A_m (cm^2)		0.011	0.023	†	−0.003	0.007	*
p_0 (mmHg)		2.2	2.46	†	0.3	2.5	NS
p_1 (mmHg)		1.8	2.03	†	−2.0	2.3	†
$C_m \left(10^{-3} \frac{\text{cm}^2}{\text{mmHg}}\right)$		−3.5	5.5	†	2.0	1.8	†

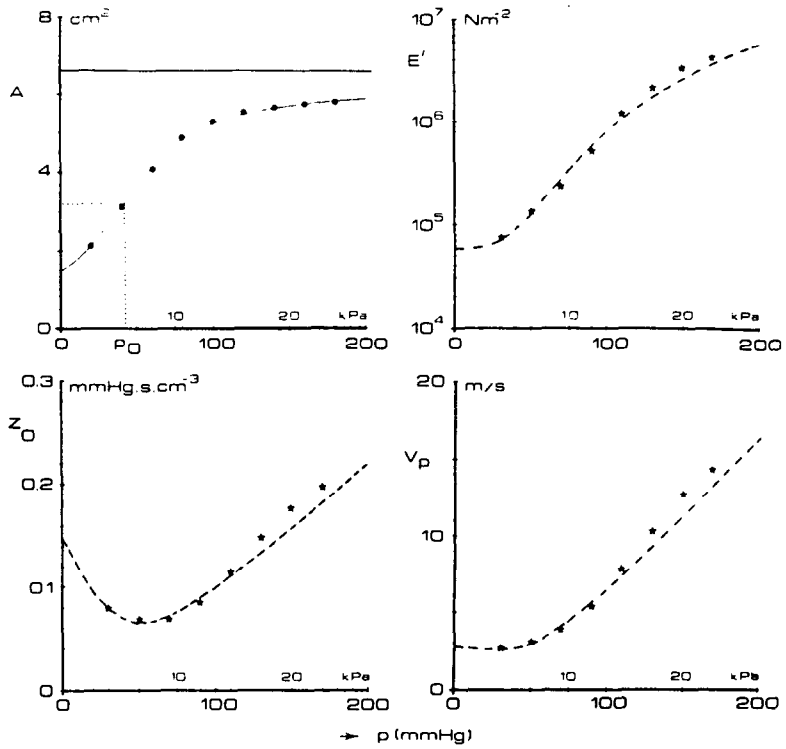

Fig. 8. The pressure–area relationship of a segment of human aorta (•) and the least squares fit of the arctangent model (solid line, equation (3)). The diagram also shows three derived quantities as a function of pressure as computed from the pressure–area data (*) and derived from the arctangent model (broken curves).

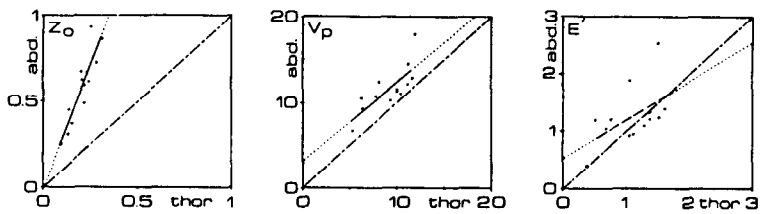

Fig. 9. Characteristic impedance, Z_0 (mmHg s cm^{-3}), pulse wave velocity, V_p (m s^{-1}), and incremental modulus of elasticity, E' (10^6 Nm^{-2}), for the abdominal aorta at 100 mmHg vs the thoracic values (13 pairs) and the linear regressions (solid lines). Dashed lines are lines of identity. The regression equations are: $Z_{0\,abd} = -0.014 + 2.88^* Z_{0\,thor}$, $r = 0.89$ ($p < 0.001$), $SEE = 0.096$, $V_{p\,abd} = 3.0 + 0.93^* V_{p\,thor}$, $r = 0.78$ ($p < 0.002$), $SEE = 1.74$, $E'_{abd} = 0.52 + 0.67^* E'_{thor}$, $r = 0.54$ (NS), $SEE = 0.44$.

relatively straight and rather uniform in diameter and wall thickness and which had only minor side branches. The magnitude of non-cylindricity was estimated by measuring some vessels a second time, rotated 90 degrees along the longitudinal axis. Results of both measurements always agreed to within 1 %.

Errors due to a natural curvature of the segments were minimized by measuring the external diameter with a balanced arrangement of two identical displacement transducers on opposite sites of the vessel. Slightly curved segments were placed in the measurement apparatus so that the curvature was in the vertical plane. Diameter changes were thus always sensed at the same points on the vessel circumference, independent of the degree of vessel distension, and only true diameter changes were measured.

End-effects due to cannulation of the segments were minimized by using segments at least 6 cm long. The influence of end-effects was studied by measuring some 10 cm thoracic segments a second time using only the middle part with a length of about 5 cm. The experimental data for two lengths always agreed to within 1 %.

Factors which might have an effect on the experimental data are

(1) temperature changes of the fluid inside the vessel segment during an experiment;

(2) time-delay between autopsy and measurement;

(3) changes in smooth muscle tone.

Visco-elastic materials possess temperature dependent

behaviour (Lawton, 1954; Apter, 1967; Cohen *et al.*, 1976). The modulus of elasticity of the aorta decreases about 4 % per degree rise in temperature (Green and Jackman, 1979). We controlled the temperature of the fluid inside the vessel segments to 37 ± 1 °C, thereby limiting the error to less than 4 %.

The influence of the time elapsed between autopsy and actual experiment was tested by repeating five measurements after storage of the segments in glucose-free Tyrode's solution at 4 °C for an additional 24 h. The repeated measurements were found to agree with the earlier measurements to within 2 %.

Following Cox (1975) we assumed that the smooth muscle in the segments was in the resting (non-contracted) state due to conditioning of the vessel segments by means of slow inflation–deflation cycles. We have not studied the effect of changes in smooth muscle tone (e.g. by norepinephrine) on the static pressure–area relationship. However, there are some reports in the literature indicating that smooth muscle contraction results in a horizontal shift of the pressure–area curve towards higher pressure levels by 10–30 mmHg (Bader and Kapal, 1963; Goedhard and Wesseling, 1976). Consequently, the max-C pressure, p_0, may increase by 10–30 mmHg due to smooth muscle contraction, whereas the parameters A_m and p_1 remain constant.

The results obtained demonstrate substantial inter-individual differences in the sizes (A, d_e) and the compliances of the aortas. In a subsequent paper we intend to show that the main part of the inter-individual variability can be 'explained' by differences in the age of the aortas. This can be judged already from the results in Tables 1, 2 and 4. In these tables the individual data of the aortic segments are presented instead of group mean values. Mean values are not considered a proper representation of the measurements in view of the large scatter, the distribution of which is quite variable as shown by the histograms below the tables. Also, measurement accuracy was high enough to let us fit our model to individual measurements rather than to group averages.

Literature data on the dimension of human arteries are scarce. Learoyd and Taylor (1966), using Bergel's technique (Bergel, 1961b), have reported data on human arterial segments from 5 anatomical locations, including thoracic and abdominal aortas and for two age groups: 'young' subjects $\leqslant$ 20 years of age; 'old' subjects > 35 years of age. Their measurements were performed at room temperature. If, for comparison, we select from our data aortas of similar age we find our values of the relative wall-thickness at 100 mmHg to be slightly greater and retraction to be slightly smaller than those reported by Learoyd and Taylor. These differences are probably significant statistically ($p = 0.05$), for which difference we have no explanation.

The three-parameter arctangent model appears to

Table 4. Hemodynamic quantities derived from the measurements and given at a pressure of 100 mmHg. These quantities are strongly pressure level dependent. See Fig. 8 for typical curves. E' = incremental Young's modulus; Z_0 = characteristic impedance; V_p = pulse wave velocity

	THORACIC AORTA					ABDOMINAL AORTA				
	patient nr.	age years	Z_0 mmHg.s/cm³	V_p m/s	E' 10^6 Nm^{-2}	patient nr.	age years	Z_0 mmHg.s/cm³	V_p m/s	E' 10^6 Nm^{-2}
•	78067	30	0.15	5.3	0.35	• 78067	30	0.17	6.6	0.39
•	78003	39	0.10	6.3	0.76	• 78003	39	0.25	9.2	1.20
	77264	45	0.15	7.1	0.74					
	78111	45	0.18	7.5	0.88	78107	40	0.50	8.4	0.89
•	78094	46	0.21	7.7	0.68	• 78094	46	0.67	10.7	1.03
	78098	47	0.12	6.7	0.85	78119	46	0.43	11.3	1.74
•	77278	50	0.14	6.2	0.51	• 77278	50	0.45	10.5	1.18
	78054	50	0.25	9.7	1.17	• 78009	53	0.31	12.4	1.87
	78080	50	0.21	9.9	1.47	• 4079	54	0.49	10.2	0.94
•	78009	53	0.13	8.1	1.06	• 77266	57	0.86	11.2	0.91
•	4079	54	0.22	9.2	1.11	78023	58	0.45	12.3	1.69
	78065	56	0.19	9.1	1.27	• 77207	59	0.62	11.5	1.20
	3972	57	0.14	8.3	0.86					
•	77266	57	0.31	10.0	1.05	78052	63	0.34	12.3	1.89
	78173	58	0.15	9.4	1.38	• 78048	64	0.59	11.0	1.23
•	77207	59	0.21	10.0	1.37	• 77286	66	0.61	12.8	1.38
	78063	60	0.18	9.7	0.97	78060	70	0.46	14.2	2.22
	78014	63	0.14	8.0	0.96	• 77196	73	0.67	14.5	1.13
•	78048	64	0.22	10.4	1.51	78182	75	0.64	14.7	1.55
	3942	65	0.14	8.8	0.86	• 77292	76	0.72	12.1	1.09
•	77286	66	0.24	11.7	1.60	• 77297	76	0.93	17.9	2.52
	77291	66	0.17	10.4	1.46	78047	78	0.62	13.5	1.79
	77296	66	0.12	9.5	1.34					
	78051	66	0.19	10.1	1.18					
	3938	68	0.19	9.0	0.95					
	4020	68	0.26	12.8	1.71					
	78032	71	0.14	9.9	1.13					
	3943	71	0.18	12.5	2.00					
	4097	72	0.25	11.5	1.58					
	78174	72	0.17	10.9	1.33					
•	77196	73	0.20	11.2	1.37					
	78185	75	0.31	17.0	4.09					
	4088	76	0.20	14.8	2.64					
•	77292	76	0.28	11.2	1.28					
•	77297	76	0.25	11.9	1.50					
	77268	79	0.18	13.2	1.80					
	77267	80	0.34	15.6	2.75					
	77285	81	0.14	13.2	2.69					
	77271	82	0.28	15.5	2.80					
	4023	85	0.21	14.8	3.20					
	4071	85	0.22	11.0	1.17					
	3971	87	0.21	13.3	1.29					
	77292	87	0.22	15.5	2.41					
	77213	88	0.20	11.2	1.52					
	77289	88	0.16	12.1	2.01					

describe the relationship between the cross-sectional area and the distending pressure well. Since three parameters were estimated from the nine measurement points this is essentially a 'smoothing' operation. For a well-behaved model the resulting parameter values are expected to have less scatter than the original measurements, allowing better conclusions to be drawn. The model allows 'interpolation' of values between the actual measurements. It also allows 'extrapolation' or 'prediction' outside the actual measurement range, although this is usually a more risky operation. However, since the arctangent model is smooth and well-behaved and fits a wide range of different pressure–area curves, moderate extrapolation seems reasonable in our case. We therefore feel justified in presenting values for p_0 that sometimes fall outside of our measurement range as do their associated p_1's. Since the arctangent function fits both human thoracic and abdominal aortic segments and since it also describes the pressure-dependent behaviour of derived hemodynamical quantities, such as compliance, characteristic impedance, etc. (Figs 4 and 8) it is presented as a suitable general 'aortic' model.

Although the arctangent model provides an adequate description, the question remains as to the uniqueness of this function. We found that other functions, such as a combination of positive and negative exponentials and a modified error function, $erf(x)$, were not able to fit the measurements as well as our model, leaving substantial systematic errors even though some of the functions tried had more than three parameters. We therefore conclude that the arctangent model provides not only an adequate but also rather unique way of summarizing the observations mathematically, based on the square law dependence of Young's modulus on pressure.

In the literature others have paid attention to the mathematical description of the mechanical properties of arteries. Wezler and Schluter (1953) proposed a power function between external radius and pressure for small arteries: $r_e = a + bp^c$ in which a, b and c are parameters. To account for the S-shaped appearance, two such functions with different parameters for different pressure regions were combined. Thus a total of four parameters was found necessary. Sinn (1956) used the power function $A = ap^{2m}$ to describe the relation between an arteries cross-sectional area and pressure. He used the data of Hallock and Benson (1937) on human arterial segments (not held at constant *in-situ* length but free to lengthen on inflation) to estimate the a and m. Here also, different values of m for different pressure regions proved necessary. A total of three parameters was thus required.

More recently, Loon *et al.* (1977), who measured the pressure–volume relationship of segments of dog and human carotid and iliac arteries held at different constant lengths, proposed the following formula for the relationship between pressure and volume $V = V_0 + (V_m - V_0)(1 - \exp(-ap))$ in which V_0 is the volume at zero pressure and V_m is the limiting value of V at high pressure levels. This formula appeared to be applicable to data of segments that were held at a length smaller than the *in-situ* length. However, if the vessel segments were held at a length near the *in-situ* length the S-shaped appearance became more pronounced, in agreement with the observations of Bergel (1960) on dog aortas, with the formula no longer applicable.

Characteristic impedance and pulse wave velocity and their pressure dependency are well predicted by the arctangent model. Substantial differences appear between the characteristic impedances for thoracic and abdominal aortas. The characteristic impedance of the abdominal aorta (at 100 mmHg) is about three times that of the thoracic aorta of the same subject (Fig. 9). This factor is related to the combination of a smaller area and a smaller compliance of the abdominal aorta

$$Z_0 = \sqrt{\rho/AC} \quad \text{with} \quad A_{(abd)} = 1/2\, A_{(thor)} \quad \text{and} \quad C_{(abd)} = 1/4\, C_{(thor)}.$$

The incremental Young's modulus, E', was not found to be significantly different for thoracic and abdominal aortas. The values reported by Learoyd and Taylor (1966) for the incremental modulus of elasticity of the thoracic aorta at 100 mmHg are about a factor of two higher than ours at comparable age, namely: 17.0×10^5 Nm^{-2} ($N = 6$) vs 8.9×10^5 Nm^{-2} ($N = 8$). Those for the abdominal aorta on the other hand are about the same, namely: 12.0×10^5 Nm^{-2} ($N = 3$) and 12.1×10^5 Nm^{-2} ($N = 5$) respectively. However, the use of the Young's modulus can be criticized, because its derivation from pressure–diameter measurements is based on a seriously invalid model for the inhomogeneous arterial wall. In particular, the percentage composition of the aortic wall and the amount of atherosclerotic deposits determine the outcome. The actual value of the Young's modulus is thus representative for nothing. It should not be used to derive quantities of hemodynamic significance, uncritically.

Richter (1980) performed pressure-volume measurements, similar to the experiments of Simon and Meyer (1958), on whole aortas (from the arch to the iliac bifurcation). He reported that the coefficient of volume elasticity of human aorta, defined as $K = V\,\Delta p/\Delta V$, ranges from 1.0×10^4 Nm^{-2} to 13.0×10^4 Nm^{-2} ($N = 58$, age range 19–74 yr). If we compute the coefficient of volume elasticity from our measurements as $K = A/C$, it ranges from 3.0×10^4 Nm^{-2} to 14.5×10^4 Nm^{-2}($N = 21$, age range 39–73 yr). These values do not differ statistically significantly from those reported by Richter. Richter also computed the compliance of the aorta (defined as $\Delta V/\Delta p$) as a function of pressure. The shape of his compliance curves are similar to ours. His compliance values cannot be compared to ours, since ours are per unit length and Richter did not report the length of his aortas.

Acknowledgements—The help of members of the pathologic anatomy departments of the OLVG (Head: Dr. E. L. Frensdorf) and the AZVU is gratefully acknowledged. We

also acknowledge the help of Mr. J. Koops of the Department of Cardiology of the State University in Leiden with respect to the impedance-rheographic measurements.

This work was supported in part by the Organization for Pure Scientific Research ZWO-FUNGO under grant no. 13-26-16.

REFERENCES

Apter, J. T. (1967) Correlation of visco-elastic properties of large arteries with microscopic structure. IV. Thermal responses of collagen, elastin, smooth muscle and intact arteries. *Circulation Res.* **21**, 901–918.

Bader, H. (1963) Anatomy and physiology of the vascular wall. *Handbook of Physiology, Circulation*, (Edited by Hamilton, W. F. and Dow, P.), Vol. II, pp. 865–891. American Physiology Society, Washington, DC

Bader, H. and Kapal, E. (1963) Vergleichende Untersuchungen ueber die Elastizitaet der Aorten verschiedener Tierarten und des Menschen. *Z. Biol.* **114**, 89–111.

Bergel, D. H. (1960) The visco-elastic properties of the arterial wall. Thesis, University of London.

Bergel, D. H. (1961a) The static elastic properties of the arterial wall. *J. Physiol.* **156**, 445–457.

Bergel, D. H. (1961b) The dynamic elastic properties of the arterial wall. *J. Physiol.* **156**, 458–469.

Bergel, D. H. (1972) The properties of blood vessels. *Biomechanics, its Foundations and Objectives*, (Edited by Fung, Y. C. B., Perrone, N. and Anliker, M.), pp. 105–139. Prentice Hall, Englewood Cliffs, NJ.

Cohen, R. E., Hooley, C. J. and McCrum, N. G. (1976) Viscoelastic creep of collagenous tissue. *J. Biomechanics* **9**, 175–184.

Cox, R. H. (1975) Anisotropic properties of the canine carotid artery *in vitro*. *J. Biomechanics* **8**, 293–300.

Dobrin, P. B. (1978) Mechanical properties of arteries. *Physiol. Rev.* **58**, 397–460.

Fung, Y. C. B. (1967) Elasticity of soft tissues in simple elongation. *Am. J. Physiol.* **213**, 1532–1544.

Fung, Y. C. B. (1972) Stress-strain-history relations of soft tissues in simple elongation. *Biomechanics, its Foundations and Objectives*. (Edited by Fung, Y. C. B., Perrone, N. and Anliker, M.), pp. 181–208. Prentice-Hall, Englewood Cliffs, NJ.

Fung, Y. C. B. (1973) Biorheology of soft tissues. *Biorheology* **10**, 139–155.

Geddes, L. A. and Baker, L. E. (1968) *Principles of Applied Biomedical Instrumentation*. John Wiley, New York.

Goedhard, W. J. A. and Wesseling, K. H. (1976) Influence of smooth muscle contraction on vascular compliance. *Proceedings of the 17th Dutch Federative Meeting*, p. 202. F.M.W.V., Nijmegen.

Green, J. F. and Jackman, A. P. (1979) Mechanism of increased vascular capacity produced by mild perfusion hypothermia in the dog. *Circulation Res.* **10**, 778–781.

Hallock, P. and Benson, I. C. (1937) Studies on the elastic properties of human isolated aorta. *J. clin. Invest.* **16**, 595–602.

Horwitz, D. L. and Homer, L. D. (1970) Analysis of biomedical data by time-sharing computers. I. Non-linear regression analysis. Naval Medical Research Institute Report no. 25.

Kapal, E. (1954) Die elastischen Eigenschaften der Aortenwand sowie des elastischen kollagenen Bindegewebes bei frequenten zyklischen Beanspruchungen. *Z. Biol.* **107**, 347–404.

Kenner, Th. (1967) Neue Gesichtspunkte und Experimente zur Beschreibung und Messung der Arterienelastizitaet. *Arch. Kreislaufforsch.* **54**, 68–139.

Krafka, J. (1939) Comparative study of the histo-physics of the aorta. *Am. J. Physiol.* **125**, 1–14.

Langewouters, G. J., Wesseling, K. H. and Goedhard, W. J. A. (1981) A new model for the static elastic properties of the aging human aorta. *Cardiovascular Physiology of the Heart, Peripheral Circulation and Methodology* (Edited by Kovach, A. G. B., Monos, E. and Rubanyi, G.) *Adv. Physiol. Sci.* **8**, 271–281.

Langewouters, G. J. (1982) Visco-elasticity of the human aorta *in vitro* in relation to pressure and age. PhD thesis, Free University, Amsterdam.

Lawton, R. W. (1954) The thermoelastic behaviour of isolated aortic strips of the dog. *Circulation Res.* **2**, 344–353.

Learoyd, B. M. and Taylor, M. G. (1966) Alterations with age in the visco-elastic properties of human arterial walls. *Circulation Res.* **18**, 278–292.

Loon, P. van, Klip, W. and Bradley, E. L. (1977) Length–force and volume–pressure relationships of arteries. *Biorheology* **14**, 181–201.

Marquardt, D. W. (1963) An algorithm for least squares estimation of non-linear parameters. *J. Soc. ind. appl. Math.* **11**, 431–441.

Remington, J. W. (1955) Hysteresis-loop behaviour of the aorta and other extensible tissues. *Am. J. Physiol.* **180**, 83–95.

Remington, J. W. (1963) The physiology of the aorta and major arteries. *Handbook of Physiology, Circulation* (Edited by Hamilton, W. F. and Dow, P.), Vol. II, pp. 799–838. American Physiological Society, Washington, D.C.

Reuterwall, O. P. (1921) Ueber die Elastizitaet der Gefasswaende und die Methode ihrer naeheren Pruefung. *Acta Med. Scand.* Suppl. **2**, 1–175.

Richter, H. A. (1980) Funktions- und Stroemungsuntersuchungen am Aortenmodell und an menschlichen Aorten in einem Kreislaufsimulator. Thesis, Technical University, Aachen (Germany).

Simon, E. and Meyer, W. W. (1958) Das Volumen, die Volumdehnbarkeit und die Druck-Laengen Beziehungen des gesamten aortalen Windkessels in Abhaengigkeit von Alter, Hochdruck und Arteriosklerose. *Klin. Wschr.* **36**, 424–432.

Sinn, W. (1956) Die Elastizitaet und ihre Bedeutung fur die Dynamik des Arteriellen System. *Abh. math.-naturw. kl. Akad. Wiss. Mainz* **11**.

Wesseling, K. H., Westerhof, N. and Sipkema, P. (1978) A 2 ms rise-time hydraulic valve. Progress Report 6, Institute of Medical Physics TNO, Utrecht (Netherlands), pp. 229–231.

Westerhof, N., Elzinga, G. and Sipkema, P. (1971) An artificial arterial system for pumping hearts. *J. appl. Physiol.* **31**, 776–781.

Wetterer, E. and Kenner, Th. (1968) *Grundlagen der Dynamik des Arterienpulses*. Springer-Verlag, Berlin-Heidelberg-New York.

Wezler, K. and Schluter, F. (1953) Die Querdehnbarkeit isolierter kleiner Arterien vom muskulaeren Typ. *Abh. math.-naturw. kl. Akad. Wiss. Mainz* **8**, 413–492.

Yin, C. P. (1980) The aging vasculature and its effect on the heart. *The Aging Heart* (Edited by Weisfeldt, M. L.), pp. 137–213. Raven Press, New York.